ChemComm

Accepted Manuscript

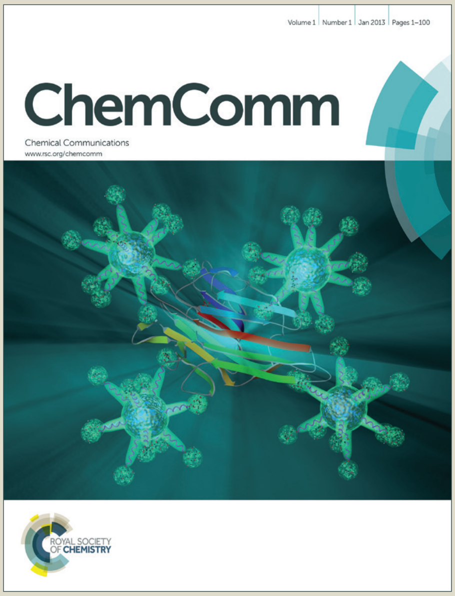

ROYAL SOCIETY OF CHEMISTRY

www.rsc.org/chemcomm

Dynamic Article Links ▶

Cite this: DOI: 10.1039/c0xx00000x

www.rsc.org/xxxxxx

ARTICLE TYPE

Novel Electrochemical Fingerprinting Methods for the Precise Determination of Pt_{Shell} Coverage on Ru_{Core} Nanoparticles

Ehab N. El Sawy[a,b], Hany A. El-Sayed[a,b], and Viola I. Birss[*a]

Received (in XXX, XXX) Xth XXXXXXXXX 20XX, Accepted Xth XXXXXXXXX 20XX

DOI: 10.1039/b000000x

The surface composition of nanoparticles is critical in defining their chemical and electrochemical properties. However, there are a limited number of tools that can rapidly and reliably establish these important characteristics at this small scale. In the present work, a series of $Ru_{core}@Pt_{shell}$ nanoparticles (2 or 3 nm diameter Ru core, 0 to 2 monolayers of Pt in the shell layer) were synthesized and several novel electrochemical fingerprinting methods were developed to determine the Pt shell characteristics. These involved tracking the charge associated with the reduction of the oxide film formed on the exposed Ru_{core}, as well as the potential and charge associated with CO_{ads} stripping, giving the precise coverage of the first and second Pt monolayer, respectively.

The catalytic properties of nanoparticles (NPs) depend on their size and composition, as well as on the population and distribution of surface sites at the atomic level[1-4]. Therefore, the ultimate goal in catalyst design is to have full synthetic control of both the bulk and surface characteristics of the catalytic material and hence on its subsequent reactivity[4].

Pt-Ru NPs, in either alloy or core@shell form, have attracted significant interest due to their many important catalytic applications, including in the electro-oxidation of methanol in direct methanol fuel cells (DMFCs)[2, 3], the preferential oxidation of CO in hydrogen feeds (PROX)[5], and the electro-oxidation of CO-contaminated hydrogen in proton exchange membrane fuel cells (PEMFCs)[6]. As a subset of Pt-Ru, Ru-Pt core-shell NPs ($Ru_{core}@Pt_{shell}$) have been reported to exhibit significantly different catalytic properties than Pt-Ru alloy NPs or mixtures of monometallic Pt and Ru NPs, due to their unique electronic characteristics[5].

Previous efforts to establish the surface composition of Pt-Ru NPs have involved the use of underpotential deposition/stripping of Cu[7, 8] and oxalic acid oxidation[9]. However, this prior work did not take into consideration the effect of NP size, Pt-Ru interactions at the surface, or the degree of Ru oxidation, on the electrochemical behavior of PtRu, thus making the conclusions drawn questionable. Also, CO stripping-voltammetry was used for the determination of the stability of PtRu NPs, including monometallic Pt and Ru, Pt-Ru alloy, and $Ru_{core}@Pt_{shell}$[10]. The change in the characteristics of the CO stripping CV peaks was used as indication for the surface composition change, and hence the stability of the different PtRu NPs[10]. In the present work, several simple, but robust, electrochemical fingerprinting methods were developed to precisely determine the coverage of both the first and second monolayer (ML) of the Pt_{shell} on the Ru_{core} particles. Specifically, the exact coverage of up to one full ML of the Pt_{shell} on the Ru_{core} was determined by monitoring the decrease in the Ru oxide (RuO_x) reduction peak in 0.5 M H_2SO_4 as the Ru core was gradually covered with the first Pt ML. To determine the coverage of the second Pt_{shell} monolayer, the difference in the electronic properties of the first Pt ML vs. the expanding second Pt ML was carefully probed by tracking the CO adsorption/stripping electrochemistry. This vital atomic level surface information would normally only be obtainable using sophisticated and costly techniques, such as synchrotron radiation based X-ray absorption spectroscopy (SR-XAS)[1, 3, 11].

The Ru_{core} NPs, ca. 2 or 3 nm in diameter (Figs. S1a and S1b), were synthesized (SI 1.1) using a simple polyol colloidal synthesis method[5, 10] in which ethylene glycol (EG) or pentamethylene glycol (PMG), respectively, were used as both the solvent and the reducing agent. The Pt_{shell}, up to two MLs in coverage, was then *controllably* deposited on the surface of Ru core NPs (for details, see SI 1.2). In order to obtain the desired coverage, the Ru:Pt atomic ratio in the synthesis solution was calculated using equation 1 (SI 1.2) and Fig. S2. The molar % Pt in the synthesis solution was found to match the Pt at% (determined using wavelength dispersive X-ray spectroscopy (WDS)) in the $Ru_{core}@Pt_{shell}$ NPs, as shown in Fig. S3. Based on the WDS results, the $Ru_{core}@Pt_{shell}$ NPs are coded as $Ru_x@Pt_y(z)$, where x and y represent the Ru and Pt at %, respectively, and z represents the coverage in number of Pt shell MLs (based on equation 1 in SI 1.2).

$Ru_{core}@Pt_{shell}$ formation was confirmed using transmission electron microscopy (TEM), coupled with energy dispersive X-ray analysis (EDX) (Fig. S4), while the $Ru_{core}@Pt_{shell}$ NP crystal structure was determined using powder X-ray diffraction (PXRD) methods. In fact, the XRD patterns of the Ru@Pt NPs (Fig. S5) are very similar to what has been reported previously for core@shell structures[12]. Also, the gradual change in the Ru crystal structure as the Pt shell coverage of the Ru core increases (Fig. S5) and the associated quantitative analysis of the XRD data (Fig. S6) are further strong evidence for $Ru_{core}@Pt_{shell}$ NP formation[12].

It is very well established that Ru has the tendency to form an ad-layer of oxygenated species when exposed to potentials of 0.2-0.9 V vs. RHE in 0.5 M H_2SO_4[13], while Pt tends to form a similar ad-layer only at > 0.8 V vs. RHE[14]. Therefore, as the Pt coverage increases on the Ru_{core} surface, the number of sites available for the formation of Ru oxide (RuO_x) should decrease, as shown in Scheme 1. This phenomenon was used here as the foundation for determining the relative surface occupation of Pt vs. Ru at the $Ru_{core}@Pt_{shell}$ NPs in the first Pt ML.

Fig. 1 shows the electrochemical response of a range of $Ru_{core}@Pt_{shell}$ NPs with an increasing Pt_{shell} coverage up to 1.1 MLs during cyclic voltammetry (CV) scans between 0.05 and 0.9 V vs. RHE in de-aerated 0.5 M H_2SO_4. In this study, the current was normalized to the total number of moles of Ru and Pt within the NPs rather than to the NP mass, because the Pt molar mass is almost twice that of Ru. Fig. 1 shows that the RuO_x reduction peak is centred at 0.25-0.35 V[13] and that it decreases in size as the Ru surface sites are blocked by the Pt shell. Further, Fig. S7 confirms that the electrochemical response depends only on the coverage of the first Pt ML, and not on the CV cycle number, thus also demonstrating the stability of the sub-monolayer Pt shell. Notably, the difference between the CV response reported here for the Ru@Pt NPs (Fig. 1) and that published for PtRu alloys[15] is further evidence of core@shell structure formation in this work. Thus, based on the reliability of the prior literature in this field[5, 12], as well as our XRD (Fig. S5 and S6) and CV (Fig. 1) results, we are certain that we have produced core@shell structures without any alloying.

The inset in Fig. 1 shows that the RuO_x reduction peak current (i_{RuOx}), which is directly proportional to the peak charge, is linearly related to the extent of coverage of Ru by the first Pt shell, calculated from the Ru NP size and the WDS-determined Pt:Ru atomic ratios. This confirms the validity of this simple electrochemical fingerprinting method to determine the coverage of the first Pt shell ML on the underlying Ru core. Importantly, once one Pt ML fully covers the Ru_{core} NPs, a RuO_x reduction peak is no longer visible (Fig. S8), as predicted.

To establish the precise coverage of the second Pt ML in the shell layer (with the Ru core now fully covered by Pt), the electrochemical oxidation of pre-adsorbed CO on Pt was tracked. It is known that the coupling between adsorbate valence states and transition metal substrate d-states defines the value of the adsorption energy[10]. Also, altering the composition and the arrangement of atoms within a NP is known to affect the electronic properties of the surface atoms and hence the characteristics of adsorption processes, such as for CO. Therefore, changes in the adsorption behaviour can be used to determine the surface composition. This concept has been used by others to monitor the stability and activity of Pt-Ru catalysts, such as alloyed Pt-Ru[16], non-alloyed Pt-Ru [17], Ru-incorporated Pt [18], Pt surface modified Ru[19], and $Ru_{core}@Pt_{shell}$ structures[10, 20]. However, the CO adsorption characteristics have not been monitored previously to serve as an indicator of the coverage of the second metal ML in a shell layer around the core of another metallic NP.

Therefore, the novel concept employed here is that, when between one and two Pt MLs are present on the Ru_{core}, there should be two distinguishable types of Pt atoms present, as shown in Scheme 2. The first (Type A) involves the full inner Pt ML, which is in direct contact with the underlying Ru_{core} atoms, while the second (Type B) is in the outer ML that is in contact with Type A Pt atoms. It is therefore expected that these two types of Pt surface atoms will have quite different electronic properties and hence should produce two types of adsorbed CO. Thus, the electrochemical fingerprint of each type of CO (and thus each type of Pt) during CO adsorption/oxidation should be easily distinguishable.

CO stripping experiments were carried out first on monometallic Ru and Pt NPs, supported on Vulcan carbon (VC) powder, with the stripping peaks seen at 0.62 and 0.83 V vs. RHE, respectively (Fig. S9). Further, when Pt and Ru NPs, on VC, were physically mixed together, a CO stripping peak is seen at each of these potentials (Fig. S9), indicating the absence of any interactions between the Ru and Pt NPs in terms of their catalytic activity towards CO adsorption or oxidation.

However, Fig. 2 clearly shows that, in the case of the $Ru_{core}@Pt_{shell}$ NPs, when the Pt coverage ranges from 0 to 1 ML, CO stripping appears as a single peak (Peak A) at a potential very close to that seen for CO stripping from pure Ru. This is consistent with the presence of only Type A Pt sites and thus only Type A adsorbed CO (Scheme 2). Under these conditions, CO oxidation is controlled entirely by strong electronic interactions between the first Pt ML in the Pt_{shell} and the Ru_{core} atoms. More importantly, this also indicates the absence of any effect of the exposed Ru surface atoms on CO oxidation, i.e., no bi-functional effect[5, 20] is observed. It should be noted that the absolute magnitude of the CO stripping peaks was not the main focus of this work, as this depends strongly on the real surface area of the NPs. This, in turn, depends on the final size and distribution of the $Ru_{core}@Pt_{shell}$ NPs. Therefore, the CO peak currents were normalized to the magnitude of the larger of the two CV peaks (Type A and Type B CO) for easier comparison.

Fig. 2 shows that, in the case of the $Ru_{48}@Pt_{52}$ (1.1) NPs, where 10% of a second ML of Pt coats the Ru core, the main CO stripping peak (peak A) is still at 0.62 V vs. RHE (Type A CO), but a small shoulder is also now seen at 0.75 V vs. RHE (peak B). In the case of $Ru_{38}@Pt_{62}$ (1.45) NPs, with 0.45 of a second Pt ML in the shell, both peaks A and B are very well-defined, consistent with the exposure of two different Pt sites to the solution (Scheme 2). These CV peaks are still better resolved at lower sweep rates (Fig. S10). When the Pt_{shell} coverage is close to 2 MLs (Fig. 2), peak B is by far the dominant feature, with only a small shoulder seen at 0.65 V vs. RHE, fully consistent with Scheme 2.

It is thus clear that, as Type A Pt atoms (Scheme 2) are in direct contact with the Ru_{core}, the CO molecules at these sites are only weakly adsorbed and thus require less energy (a lower potential) to be oxidized (Peak A in Fig. 2). However, at Type B Pt sites, where the electronic effect of Ru on the surface Pt atoms is buffered by the presence of an under-layer of Pt [21], CO stripping should be energetically more difficult, consistent with the higher CO stripping potential observed (Peak B, Fig. 2).

In the case of $Ru_{38}@Pt_{62}$ (1.45), the surface fraction of Type A and Type B Pt should be 0.55 and 0.45, respectively, and hence the ratio of Peak A to Peak B is expected to be 1:0.82, assuming that the peak current is directly related to the CO coverage at each Pt type. The experimental ratio of Peak A:Peak B was found to be very similar to this, i.e., 1:0.88 (Fig. 2), indicating the excellent precision of this electrochemical fingerprinting method for the determination of the coverage of the second Pt ML in the Pt_{shell}. Also, in the case of the $Ru_{48}@Pt_{52}$ (1.1) and $Ru_{31}@Pt_{69}$ (1.9) NPs, the fraction of Type B and Type A Pt atoms should be ca. 0.1, respectively. The appearance of small shoulders (arrows, Fig. 2) in the Peak B and A regions in Fig. 2 for the 1.1 and 1.9 ML cases, respectively, demonstrates the excellent sensitivity of the CO adsorption/stripping method for the determination of the Ru@Pt surface composition.

Since CO oxidation at Pt NPs is known to depend on the particle size (2-5 nm)[22], it is important to prove that the CO stripping method proposed here is independent of the Ru_{core} ($Ru_{core}@Pt_{shell}$) size. Pentamethylene glycol (PMG), which has a higher boiling point than ethylene glycol (EG), was thus used to synthesize larger Ru NPs. Fig. S11 shows that a single CO stripping peak is seen at 0.62 V vs. RHE in both cases when one Pt ML is present on the Ru_{core}. When the Pt_{shell} thickness was increased to ca. 1.5 MLs ($Ru_{38}@Pt_{62}$ (1.45, EG) and $Ru_{51}@Pt_{49}$ (1.5, PMG)), two CO stripping peaks are seen (Fig. S11), independent of the Ru_{core} size. This demonstrates the reliability of the CO stripping fingerprinting method as a surface composition characterization tool for Ru@Pt NPs of all sizes.

A theoretical calculation of the binding energy of CO on Pt showed that it should increase dramatically when the number of Pt MLs on Ru increases from 1 to 2 MLs[21], consistent with Fig. 2. Importantly, when the number of Pt MLs on Ru is increased from 2 to 3 MLs or more, the CO/Pt binding energy should hardly change[21] and thus the CO stripping method is expected to be invalid under these conditions.

In conclusion, we have developed two simple but robust electrochemical fingerprinting methods to precisely determine the surface composition of catalytic $Ru_{core}@Pt_{shell}$ NPs, formed using a simple polyol colloidal synthesis method. The coverage of the Pt_{shell} layer on top of the Ru_{core} (2-3 nm dia) can now be reliably determined. Specifically, the signal obtained from the reduction of Ru oxide, present on the uncovered Ru atoms, was used to determine the precise coverage of a first Pt shell layer, while the current and potential of the CO stripping peaks are highly reliable predictors of the coverage of the second Pt_{shell} layer.

The two electrochemical fingerprinting methods developed here should be relatively easy to extend to other core/shell N@M (N = Ru, Ni, and Co, and M = Pt, Pd and Au) structures. To determine the coverage up to 1 ML, the core material should have the ability to form a reversible oxide in a potential range different from that of the shell material, while to determine the shell coverage for >1 ML, the core material should exert a strong electronic effect on the shell, hence altering the strength of CO adsorption.

Notes and references

[a] *Department of Chemistry, University of Calgary, 2500 University Drive NW, Calgary, Alberta, Canada T2N 1N4. Phone: (403) 220-6432. Fax: (403) 289-9488, E-mail: birss@ucalgary.ca*

[b] *Permanent address: National Research Center, Dokki, Cairo, Egypt*

† Electronic Supplementary Information (ESI) available: Experimental Procedures, TEM, EDX and XRD analyses, and further CVs. See DOI: 10.1039/b000000x/

We are very grateful to the Natural Sciences and Engineering Research Council of Canada (NSERC) through its Discovery Grant and CRD granting programs, for the overall support of this work. We also thank Dr. Tobias Fürstenhaupt (Microscopy and Imaging Facility (MIF), University of Calgary) for help with the TEM/EDX analyses and Dr. Robert A. Marr (University of Calgary Laboratory for Electron Microprobe Analysis (UCLEMA)) for assistance with the WDS analyses.

1. B.-J. Hwang, L. S. Sarma, C.-H. Chen, C. Bock, F.-J. Lai, S.-H. Chang, S.-C. Yen, D.-G. Liu, H.-S. Sheu and J.-F. Lee, *The Journal of Physical Chemistry C*, 2008, **112**, 19922-19929.
2. T.-Y. Jeon, K.-S. Lee, S. J. Yoo, Y.-H. Cho, S. H. Kang and Y.-E. Sung, *Langmuir*, 2010, **26**, 9123-9129.
3. T.-Y. Chen, T.-L. Lin, T.-J. M. Luo, Y. Choi and J.-F. Lee, *ChemPhysChem*, 2010, **11**, 2383-2392.
4. P. Strasser, S. Koh, T. Anniyev, J. Greeley, K. More, C. Yu, Z. Liu, S. Kaya, D. Nordlund, H. Ogasawara, M. F. Toney and A. Nilsson, *Nat Chem*, 2010, **2**, 454-460.
5. S. Alayoglu, A. U. Nilekar, M. Mavrikakis and B. Eichhorn, *Nat Mater*, 2008, **7**, 333-338.
6. Y. Ra, J. Lee, I. Kim, S. Bong and H. Kim, *Journal of Power Sources*, 2009, **187**, 363-370.
7. C. L. Green and A. Kucernak, *The Journal of Physical Chemistry B*, 2002, **106**, 1036-1047.
8. C. N. Van Huong and M. J. Gonzalez-Tejera, *Journal of Electroanalytical Chemistry and Interfacial Electrochemistry*, 1988, **244**, 249-259.
9. C. Bock and B. MacDougall, *Journal of The Electrochemical Society*, 2003, **150**, E377-E383.
10. P. Ochal, J. L. Gomez de la Fuente, M. Tsypkin, F. Seland, S. Sunde, N. Muthuswamy, M. Ronning, D. Chen, S. Garcia, S. Alayoglu and B. Eichhorn, *J. Electroanal. Chem.*, 2011, **655**, 140-146.
11. A. Bianconi, *Applications of Surface Science*, 1980, **6**, 392-418.
12. S. Alayoglu, P. Zavalij, B. Eichhorn, Q. Wang, A. I. Frenkel and P. Chupas, *ACS Nano*, 2009, **3**, 3127-3137.
13. S. Hadzi-Jordanov, H. Angerstein-Kozlowska, M. Vukovic and B. E. Conway, *Journal of The Electrochemical Society*, 1978, **125**, 1471-1480.
14. J. Mozota and B. E. Conway, *Electrochimica Acta*, 1983, **28**, 1-8.
15. G. A. Camara, R. B. de Lima and T. Iwasita, *Electrochemistry Communications*, 2004, **6**, 812-815.
16. J. Solla-Gullon, F. J. Vidal-Iglesias, V. Montiel and A. Aldaz, *Electrochimica Acta*, 2004, **49**, 5079-5088.
17. M. Inoue, T. Nishimura, S. Akamaru, A. Taguchi, M. Umeda and T. Abe, *Electrochimica Acta*, 2009, **54**, 4764-4771.
18. J. C. Davies, B. E. Hayden and D. J. Pegg, *Surface Science*, 2000, **467**, 118-130.
19. S. R. Brankovic, N. S. Marinkovic, J. X. Wang and R. R. Adzic, *J. Electroanal. Chem.*, 2002, **532**, 57-66.
20. D. Bokach, J. L. G. de la Fuente, M. Tsypkin, P. Ochal, I. C. Endsjø, R. Tunold, S. Sunde and F. Seland, *Fuel Cells*, 2011, **11**, 735-744.
21. A. Schlapka, M. Lischka, A. Gross, U. Kasberger and P. Jakob, *Phys. Rev. Lett.*, 2003, **91**, 016101.
22. F. Maillard, E. R. Savinova and U. Stimming, *J. Electroanal. Chem.*, 2007, **599**, 221-232.